

Simulation of rock mass strength anisotropy and scale effects using a Ubiquitous Joint Rock Mass (UJRM) model

B. Sainsbury

Itasca Australia Pty Ltd, Melbourne, Australia

M. Pierce

Itasca Consulting Group Inc, Minneapolis, MN, USA

D. Mas Ivars

Itasca Geomekanik AB, Solna, Sweden

ABSTRACT: Some of the most challenging aspects of design in moderately to heavily jointed rock masses relate to the impacts of in-situ joint fabric on rock mass behavior. Preferred joint orientations can induce a marked anisotropy in modulus, strength and brittleness. In addition, joint density and persistence must be considered relative to problem size, as rock mass properties can exhibit significant scale dependence. Synthetic Rock Mass (SRM) testing provides a means to study these effects in simulated rock mass samples on the scale of 10 to 100 meters. This paper focuses on a technique to account for strength anisotropy and scale effects (as quantified through SRM testing) within large-scale *FLAC^{3D}* continuum models. This follows the work of Clark (2006), who used *FLAC* to demonstrate that the assignment of ubiquitous joint orientations at the zone level (from a known joint-orientation distribution) results in realistic rock mass behavior and yields properties that are consistent with empirical techniques. The resulting calibrated *FLAC^{3D}* material incorporates several key behaviors obtained from SRM testing and can be used in large-scale continuum models for analysis and design.

1 INTRODUCTION

The strength and deformation behavior of a jointed rock mass is governed strongly by (a) the intact strength of the rock and (b) the presence of joints/discontinuities. Synthetic Rock Mass Modeling (SRM) has been developed (Mas Ivars 2008) to allow for the detailed consideration of the rock mass joint fabric in the determination of rock mass strength at large scales – i.e. 10 to 100 m. The SRM methodology uses the Particle Flow Code *PFC^{3D}* (Itasca, 2007) to explicitly represent a discrete fracture network (DFN) embedded within an intact rock matrix. The resulting SRM can explicitly account for the presence of intact rock bridges between terminating fractures – similar to in-situ rock mass conditions. Through simulated testing of these synthetic materials, it is possible to derive rock mass properties such as modulus, strength and brittleness. At present, it is not practical to simulate large-scale mining/geological processes within *PFC^{3D}* due to the computational intensity of the numerical technique. For this reason, continuum codes such as *FLAC^{3D}* (Itasca 2006) are required to ensure reasonable computation times.

This paper describes a methodology that is used to derive material input properties for the *FLAC^{3D}* Subiquitous (Strain-Softening Ubiquitous Joint) constitutive model so that it exhibits strength and deformation behaviors similar to what may be derived from SRM testing. This methodology has been applied to four lithologies present at Rio Tinto's Palabora Mine in South Africa. The resultant *FLAC^{3D}* modeling methodology has been termed a Ubiquitous Joint Rock Mass (UJRM) model.

2 DEVELOPMENT OF A UBIQUITOUS JOINT ROCK MASS (UJRM) MODEL

2.1 The Subiquitous (Strain-Softening Ubiquitous Joint) constitutive model

The Subiquitous constitutive model in *FLAC^{3D}* is routinely used to represent laminated materials that exhibit nonlinear material hardening or softening. Clark (2006) used *FLAC* (Itasca 2005) to demonstrate that the assignment of ubiquitous joint orientations at the zone level (from a known joint-orientation distribution) results in realistic rock mass behavior and can yield properties that are consistent with empirical techniques. The methodology detailed by Clark (2006) has been extended to *FLAC^{3D}* to allow for the characterization of strength anisotropy and sample scale effects.

Within the Subiquitous constitutive model, both matrix and joint properties are specified (see Fig. 1). In order for the UJRM testing methodology to be practical and honor existing rock mechanics relations, it has been assumed that the matrix and joint properties can be derived directly from the intact or SRM testing results. By modifying these input strength parameters, the calibration of Young's Modulus, unconfined compressive strength (UCS), tensile strength and the softening behavior of different sample sizes, in different loading directions have been completed. In addition, SRM failure mechanisms within the UJRM samples also have been honored through the monitoring of progressive matrix degradation, joint slip and joint dislocation. An example of the damage propagation behaviors within a UJRM sample can be seen through the progressive degradation of matrix cohesion and ubiquitous joint-failure plots at various stages of UJRM UCS sample loading – illustrated in Figure 2.

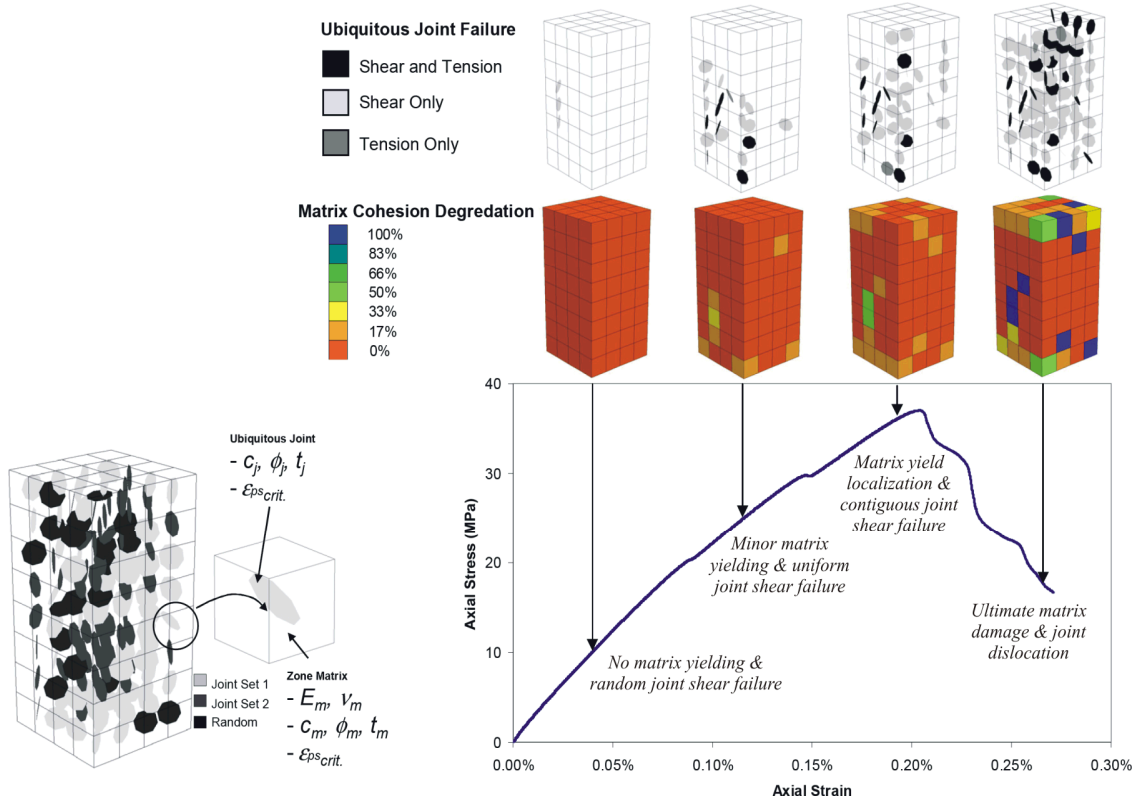


Figure 1. UJRM model: matrix and joint properties.

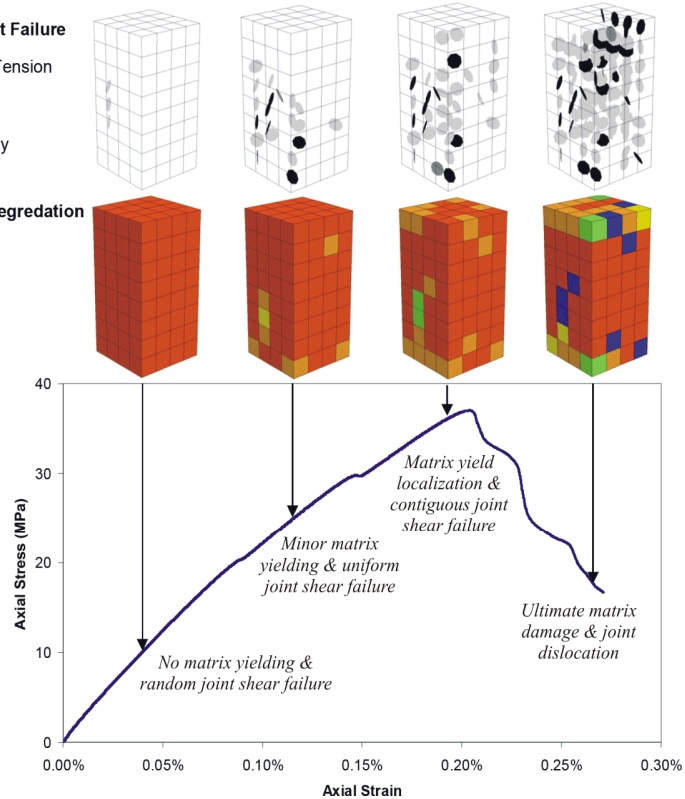


Figure 2. Stages of damage within a UJRM specimen.

2.2 Establishment of a standard UJRM laboratory testing environment

To date, SRM testing has been performed on one sample size that has been subjected to one stress-path loading condition that simulates the expected stress path *in situ*. This has made the material properties derived from this technique specific to one application. As discussed in Mas Ivars et al. (2008), the SRM methodology has been developed further to achieve calibration of the rock mass (a) in three opposing loading directions, and (b) at a number of different scales. This ensures that the material properties derived from the technique are not specific to one particular stress path and may

be applied to a number of different numerical modeling applications (i.e. cave analysis, slope stability). Commensurate with the development of the SRM standard suite of laboratory tests, UJRM testing environments (direct tensile test, uniaxial compressive strength test and triaxial test) have also been developed in *FLAC^{3D}*.

2.3 UJRM sample geometry and generation

2.3.1 Sample shape

A rectangular sample shape has been used for the generation of each UJRM test sample. This shape:

- matches the shape and volume of the SRM samples that have been tested (40 m × 40 m × 80 m, 20 m × 20 m × 40 m, and 10 m × 10 m × 20 m) – see Figure 3;
- ensures ease associated with the scaling of critical strain values during the subsequent modeling process;
- ensures ease associated with applying stresses in all three axial directions (σ_{xx} :E-W, σ_{yy} :N-S, σ_{zz} :vertical) during the laboratory testing process;
- minimizes end effects.

Figure 4 illustrates the simulated axial loading conditions for each of the UCS, triaxial and direct tension tests, and the three sample orientations tested in each environment.

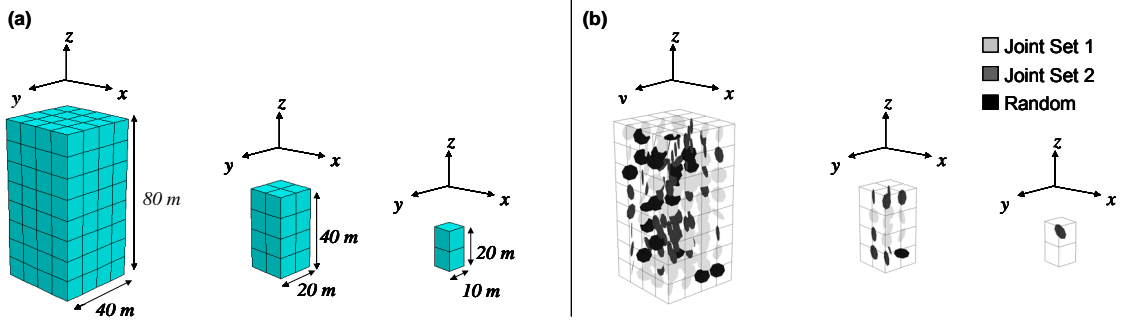


Figure 3. (a) Variation in sample size with equal zone sizes; (b) joint assignment as a function of sample size.

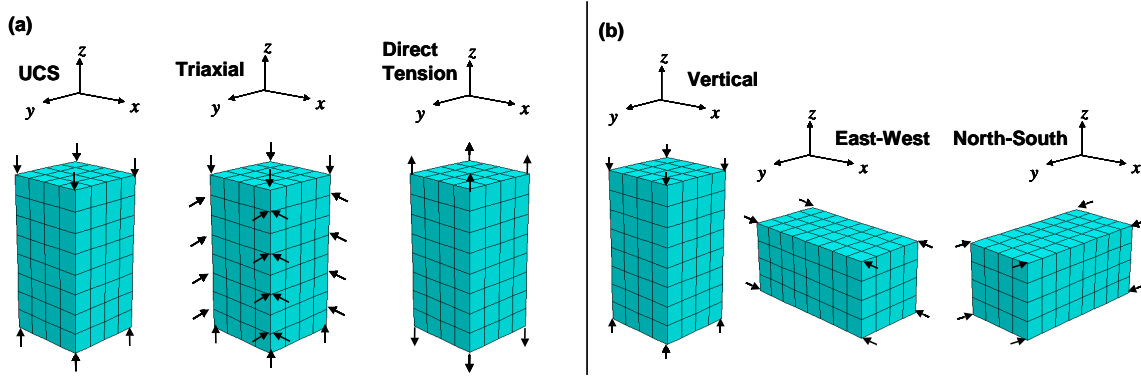


Figure 4. (a) Sample loading conditions; (b) orientation for anisotropy tests.

2.3.2 Effect of sample zone resolution

A standard zone size of 10 m × 10 m × 10 m has been selected for the generation of each sample geometry. This zone size has been selected because it matches the desired shape and size of zones to be used within large-scale *FLAC^{3D}* models. It can be seen from Figure 3 that the number of zones in UJRM test samples decreases from 128 in the 40 m × 40 m × 80 m size down to just 2 in the 10 m × 10 m × 20 m sample size. Issues associated with shear band localization within the matrix material of samples, with a coarse zone resolution (i.e. small number of zones) needs to be considered when interpreting the response of each test sample and the development of large-scale mining models. This resolution dependency has been investigated by conducting UCS tests on the various UJRM sample zone resolutions. No ubiquitous joints have been simulated during these tests. Figure 5a

illustrates the UCS stress–strain response of samples with a strain-softening (critical plastic strain > 0) matrix material. It can be seen that, with decreasing zone resolution, the post-peak response becomes more ductile. In addition, in order to generate a realistic failure mechanism, a sample with at least 10 zones across the width is required. To minimize this zone resolution dependency, illustrated in Figure 5b, the UJRM material has been calibrated with the same zone size as those used in the large mining-scale models.

2.3.3 Effects of sample loading conditions

Laboratory UCS tests conducted on intact samples are performed by loading the sample between two steel platens. These platens provide a small amount of confinement to the test specimen due to frictional resistance. In *FLAC^{3D}*, the sample loading conditions may be modeled by (a) allowing the sample ends to move in all directions perpendicular to the loading direction, (b) fixing the sample ends in all directions, or (c) modeling the steel platens above and below the sample, and installing an interface between the two materials that is assigned a stiffness and frictional resistance. The effect of each of these loading conditions on the UJRM response is shown in Figure 6. Based on the results of these tests, it can be seen that the end conditions can have a significant effect on the peak strength of the UJRM sample. To be consistent with the end conditions used throughout the SRM testing, fixed end conditions have been applied in the UJRM testing environment.

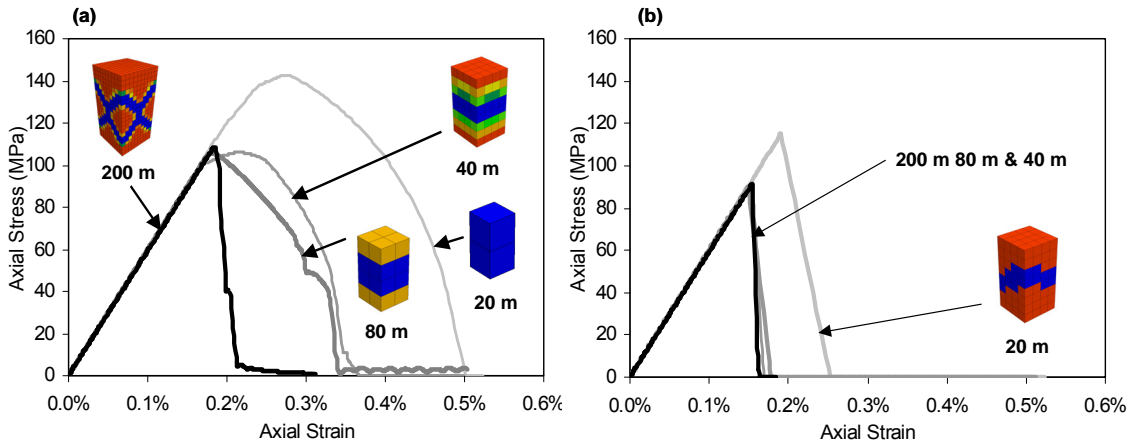


Figure 5. UJRM response as a function of zone resolution (as controlled by sample width) and assigned matrix critical strain: (a) critical strain > 0.0; (b) critical strain = 0.0.

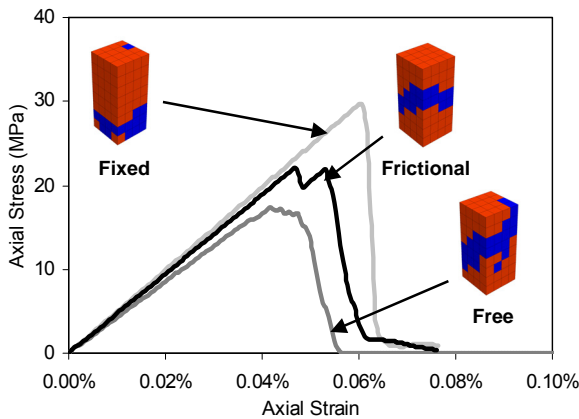


Figure 6. Simulation of different boundary loading conditions on the response of UJRM material in the UCS test environment.

2.3.4 Effect of large strain/small strain calculation model

FLAC^{3D} is able to calculate numerical solutions in both a large-strain and small-strain mode. In small-strain mode, gridpoint coordinates are not updated during mechanical calculations; in large-strain mode, gridpoint coordinates are updated at each step. The application of small-strain mode is

most useful when controlling boundary and applied conditions when large displacements are expected in relation to the grid size. In most large-scale cave analyses, small-strain mode is utilized. The effect of each of these calculation modes on the behavior of a UJRM sample has been investigated by conducting a series of UCS tests on a material that has varying joint orientations. The results are summarized in Figure 7.

It can be seen that small-strain and large-strain calculation modes yield the same results for those samples that have horizontal and random joints sets. However, significant differences in the peak and residual strengths are apparent in the sample that has a vertical joint set. The small-strain sample has much higher peak strength. The large-strain sample yields in tension along the joint surfaces and, as expected, progresses to a fully degraded state with the continued application of load. In order to allow for very large displacements in *FLAC^{3D}*, the UJRM rock mass has been calibrated using the small-strain calculation mode. This was required due to the implementation of the rock properties derived from this technique in subsequent large-scale mining numerical models.

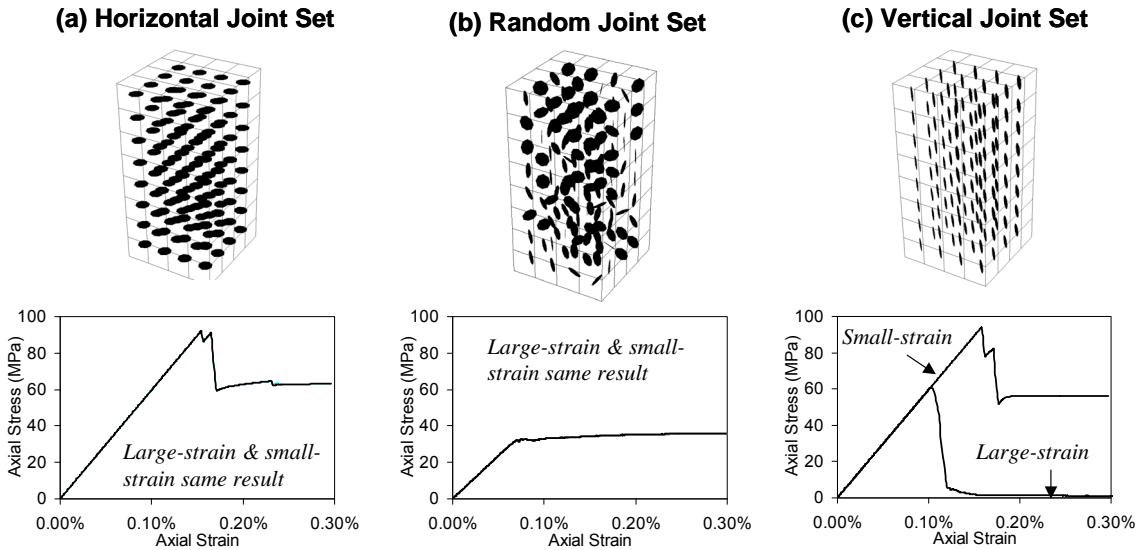


Figure 7. Investigation of UJRM response as a result of small-strain/large-strain calculation modes.

2.3.5 Simulation of discrete fracture network

Fractures are represented within the *FLAC^{3D}* sample as ubiquitous joints. The assignment of the joint dip, dip direction and radius has been achieved via a random sampling procedure from the DFN developed for the rock mass (Mas Ivars et al. 2008). The persistence of joints has been honored throughout the *FLAC^{3D}* grid via extrapolating the joint dip and dip direction to adjoining zones, which honors the fracture radius. The DFN was regenerated for each UJRM test to ensure that the strength parameters derived were representative of an average rock mass and were not dominated by a specific joint location and orientation (see Fig. 4b). An example of the ubiquitous joint orientations represented in a UJRM sample by this sampling procedure is provided in Figure 8. A summary of the joint orientations represented in each lithology DFN is provided in Figure 9.

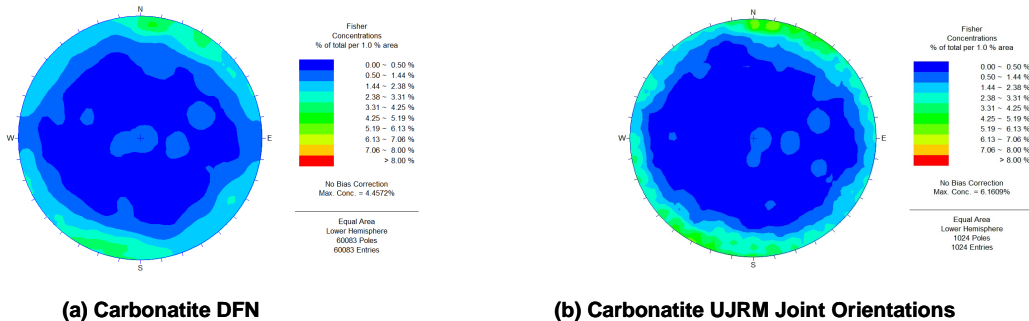


Figure 8. (a) DFN for Carbonatite; (b) Ubiquitous joint network generated in *FLAC^{3D}* for Carbonatite.

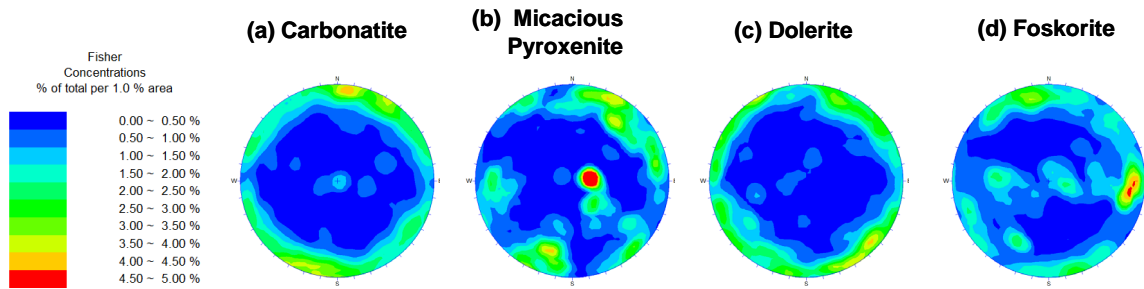


Figure 9. Joint orientations considered in the development of the DFN for (a) Carbonatite; (b) Micaceous Pyroxenite; (c) Dolerite; and (d) Foskorite.

3 SYNTHETIC ROCK MASS (SRM) TESTING RESULTS

SRM testing has been conducted on a number of rock masses that exhibit significant strength anisotropy and scale effects. These characteristics are a result of varying persistent fracture networks. A discussion of the development of the fracture networks and detailed SRM methodology can be found within these proceedings in Mas Ivars et al. (2008). Summaries of the intact and SRM-derived properties are provided in Tables 1 & 2. Results of the SRM testing show a significant strength anisotropy and scale effect in all testing directions. The results of the SRM tests have been used, along with the laboratory-derived intact properties, to calibrate a UJRM model for each of the units.

Table 1. Laboratory derived intact rock properties.

| Lithology | UCS (MPa) | Young's Modulus (GPa) | Poisson's ratio |
|----------------------|-----------|-----------------------|-----------------|
| Carbonatite | 139 | 58 | 0.33 |
| Micaceous Pyroxenite | 90 | 72 | 0.35 |
| Foskorite | 63 | 78 | 0.27 |
| Dolerite | 320 | 90 | 0.30 |

Table 2. SRM-derived strengths - Triaxial 5-MPa Confinement (MPa)

| | N-S | | | E-W | | | Vertical | | |
|----------------------|--------------|------|------|--------------|------|------|--------------|------|------|
| | Sample Width | | | Sample Width | | | Sample Width | | |
| | 40 m | 20 m | 10 m | 40 m | 20 m | 10 m | 40 m | 20 m | 10 m |
| Carbonatite | 65 | 60 | 69 | 38 | 42 | 61 | 45 | 38 | 46 |
| Micaceous Pyroxenite | 56 | | | 39 | | | 41 | 47 | 58 |
| Foskorite | 38 | 38 | 36 | 39 | 35 | 33 | 27 | 28 | 29 |
| Dolerite* | 66 | 70 | 78 | 68 | 79 | 104 | 61 | 62 | 100 |

* Dolerite samples were tested at 10 m, 5 m and 2.5 m sample sizes

4 UJRM CALIBRATION OF PALABORA LITHOLOGY SRM TESTING

A series of *FLAC^{3D}* UJRM laboratory tests has been conducted to calibrate the response of SRM laboratory-test results conducted on four lithologies present at the Palabora Mine. The following section outlines the methodology for the selection of the input parameters for calibration of the UJRM model to the SRM responses for each of the rock mass units detailed in Mas Ivars et al. (2008).

4.1 UJRM matrix properties

4.1.1 Young's Modulus and Poisson's ratio

The SRM testing considered an intact rock block Young's modulus based on laboratory testing of intact samples. When the joints were embedded within the SRM sample, the average Young's modulus decreased. In order to match the SRM-derived rock mass moduli for each UJRM, the Young's Modulus was decreased from the initial intact value. Values between 30% and 50% of the intact Young's Modulus were required to achieve calibration with the SRM samples. A summary of the calibrated moduli values is provided in Table 3.

4.1.2 Friction, Cohesion and Tension

Rock mass friction, cohesion and tension were selected based on a calibration of the UJRM matrix material to the intact rock block strength (80% of laboratory UCS strength) of each rock mass (Mas Ivars 2008). For simplicity, it was assumed that matrix friction softened to the residual joint friction angle: determined for the SRM testing. Tension softening of the matrix material has been assumed to be perfectly brittle. A dilation angle of 10 degrees was used for all rock mass simulations. A summary of the cohesion, friction and tension values required to calibrate the intact material response for each rock mass are provided in Table 3.

4.2 UJRM joint properties

4.2.1 Cohesion

Along with critical strain values, joint cohesion was varied to achieve a match in peak strength between the SRM and UJRM materials. Joint cohesions between 0.1% and 1% of the matrix cohesion were required. A summary of the joint cohesion values required to calibrate the rock mass response for each lithology is provided in Table 3.

4.2.2 Friction

Joint friction angles were set for each lithology based on estimates determined for SRM testing. For simplicity, it was assumed that joint friction did not soften. A summary of the friction values used in each UJRM calibration is provided in Table 3.

4.2.3 Tension

Joint tension was assumed to be zero for each UJRM models.

4.3 Critical Strain

Both matrix and joint critical strain values were varied to achieve calibration of the rock mass materials. Matrix critical strains ($\epsilon_{ps_{crit}}$) values between 0.01 and 0.15 were required and joint critical strains ($\epsilon_{ps_{j_{crit}}}$) less than 1% of the matrix value were required to achieve calibration of each UJRM. A summary of the critical strain values required to calibrate each rock mass is provided in Table 3.

Table 3. Calibrated UJRM and SRM Properties

| | | Carbonatite | Foskorite | Micaceous Pyroxenite | Dolerite |
|---------------|---|-------------|-----------|-------------------------|----------|
| <i>Matrix</i> | Modulus (% Intact value) | 50% | 50% | 30% | 30% |
| | Cohesion (MPa) | 15 | 7 | 10 | 37 |
| | Tension (% of Cohesion) | 40% | 40% | 36% | 56% |
| | Friction (Degrees) | 40 | 35 | 49 | 47 |
| | $\epsilon_{ps_{crit}}$ | 0.15 | 0.1 | 0.015 | 0.025 |
| <i>Joint</i> | Cohesion (% of Matrix Cohesion) | 1% | 0.1% | 0.2% | 0.1% |
| | Friction (Degrees) | 30 | 30 | 34 | 26 |
| | $\epsilon_{ps_{j_{crit}}}$ (% of $\epsilon_{ps_{crit}}$) | <1% | <1% | <1% | <1% |

4.4 Calibrated UJRM model results

Calibration of a UJRM for the Carbonatite lithology has been completed in three different testing environments, in three loading directions, and at three different scales. The resulting UJRM exhibits trends in variability, anisotropy and scale dependence that are similar to the SRM. As shown in Figure 10, the UJRM is capable of reproducing the anisotropy in peak strengths as well as the ductile stress-strain response observed during testing of the equivalent 40 m wide SRM samples. When the result of UCS tests at other scales are compared for both the SRM and UJRM (Fig. 11), it is evident that the impact of scale on the average strength and on the variability in strength is stronger in the UJRM model than in the SRM model. This can be attributed to the minimal number of joints (two) represented in these samples compared to a SRM sample. Calibrated triaxial compression results at 5 MPa confinement for each rock mass lithology are provided in Figure 12.

4.5 Discussion of test results

Based on these initial calibrations, the joint cohesion, critical strain and matrix Young’s Modulus are observed to have the most significant effect on the accuracy of the calibration.

In order to further understand the application of this methodology in large-scale mining/geological models, a detailed sensitivity study associated with each matrix and joint input parameter is required. Additional testing is also required to explore factors that might allow for greater control over the scale effects within the UJRM model. This study forms part of ongoing research funded by the Mass Mining Technology (MMT) project.

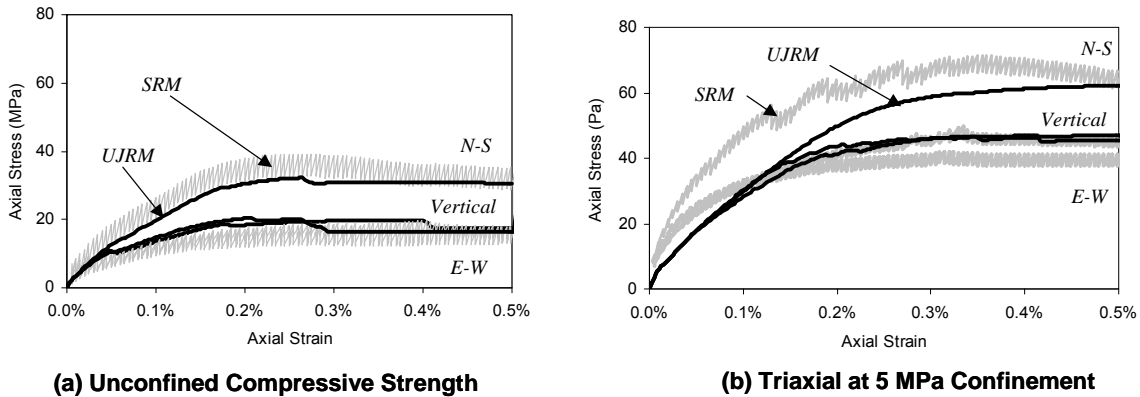


Figure 10. (a) Calibrated 40 × 80 m carbonatite UCS UJRM rock mass samples showing strength anisotropy; (b) Calibrated 40 × 80 m carbonatite triaxial UJRM rock mass samples showing strength anisotropy.

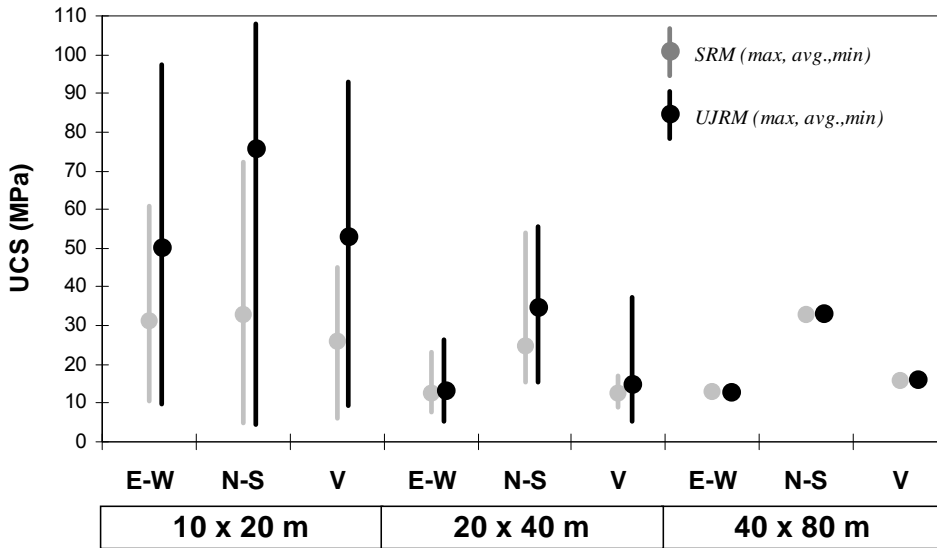


Figure 11. UJRM carbonatite UCS results compared to SRM carbonatite UCS results at three different sample sizes in three loading directions.

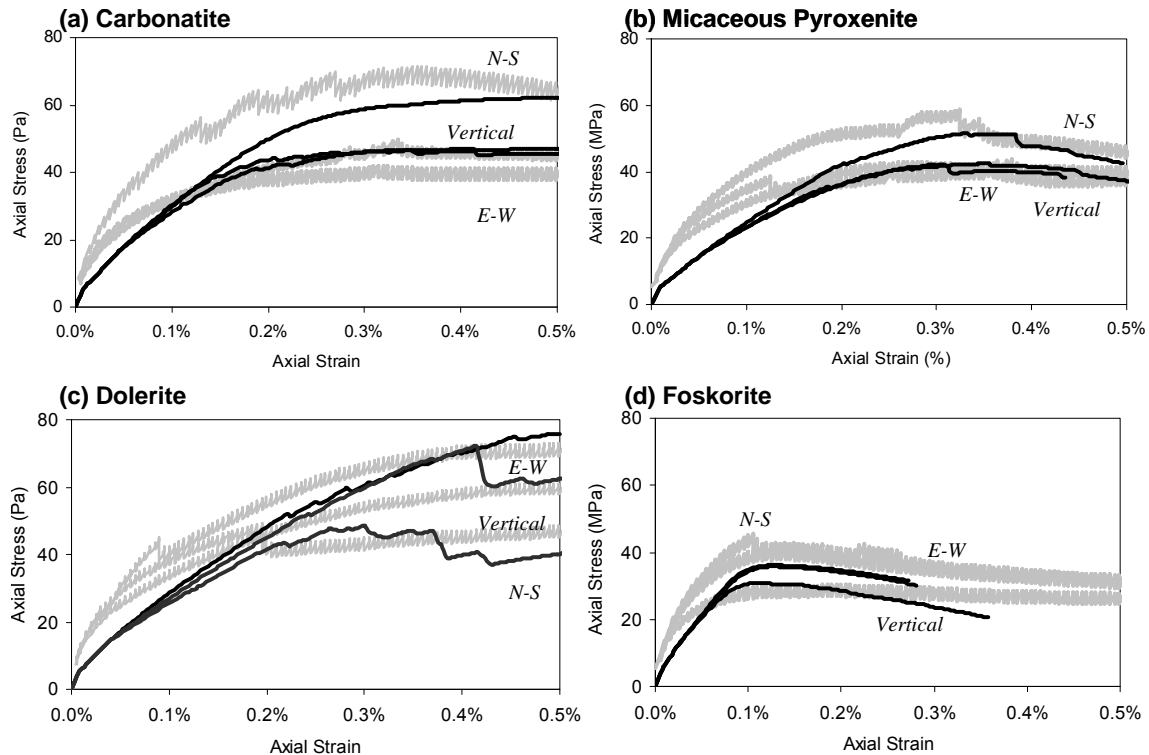


Figure 12. Calibrated UJRM: SRM results at 5 MPa confinement for each lithology in three testing directions.

5 CONCLUSIONS

Calibration of the UJRM assumes that the SRM testing is an accurate representation of the rock mass strength and deformation behavior in the tested loading directions and sample scales. Based on an initial calibration to SRM test results for lithologies at the Palabora Mine, it has been shown that the UJRM method can reproduce accurate failure mechanisms and strength anisotropy as well as some scale effects.

Prior to extrapolating UJRM models to simulation of large-scale mining /geological processes, a methodical procedure is required to validate the technique. This should include detailed back-analysis of observed failure mechanisms.

ACKNOWLEDGEMENTS

The authors wish to acknowledge the members of the MMT project for sponsoring the development of the extended UJRM method and the study case presented in this paper. In addition, we thank Caroline Darcel (Itasca Consultants S.A.S., Lyon, France) for the development of the DFN's.

REFERENCES

- Clark, I.H. 2006. Simulation of Rockmass Strength Using Ubiquitous Joints. In: R. Hart & P. Varona (eds), *Numerical Modeling in Geomechanics — 2006; Proc. 4th International FLAC Symposium, Madrid, May 2006*. Paper No. 08-07, Minneapolis: Itasca.
- Itasca Consulting Group, Inc. 2005. *FLAC – Fast Lagrangian Analysis of Continua, Ver. 5.0, User's Manual*. Minneapolis: Itasca.
- Itasca Consulting Group, Inc. 2006. *FLAC^{3D} – Fast Lagrangian Analysis of Continua in 3 Dimensions, Ver. 3.1, User's Manual*. Minneapolis: Itasca.

- Itasca Consulting Group, Inc. 2007. *PFC^{3D} – Particle Flow Code in 3 Dimensions, Ver. 4.0 pre-release*. Minneapolis: Itasca.
- Mas Ivars, D., Pierce, M., DeGagné, D. & Darcel, C. 2008. Anisotropy and scale dependency in jointed rock mass strength – A synthetic rock mass study. In R. Hart, C. Detournay & P. Cundall (eds), *Proceedings of the 1st International FLAC/DEM Symposium on Numerical Modeling, August 25-27, 2008, Minneapolis, MN USA*. Minneapolis: Itasca (In press).